

Low-frequency dynamic hysteresis in exchange-coupled $\text{Ni}_{81}\text{Fe}_{19}/\text{Ir}_{22}\text{Mn}_{78}$ bilayers

Haiwen Xi* and Robert M. White

Data Storage Systems Center, Carnegie Mellon University, Pittsburgh, Pennsylvania 15213

Sining Mao, Zheng Gao, Zhijun Yang, and Edward Murdock

Recording Head Operations, Seagate Technology, 7801 Computer Avenue South, Minneapolis, Minnesota 55345

(Received 20 February 2001; published 18 October 2001)

The dynamics of hysteresis, including the training effect, the field sweep rate dependence, and the field strength dependence of the exchange bias and coercivity, is experimentally investigated in exchange-coupled $\text{Ni}_{81}\text{Fe}_{19}/\text{Ir}_{22}\text{Mn}_{78}$ bilayers in the low-frequency range. The dependence of the exchange field and the coercivity with the number of measurement cycles is well described by a power-law function in which the index varies with the $\text{Ir}_{22}\text{Mn}_{78}$ thickness. We have also found that the exchange bias depends upon the sweep rate according to a power law. This “training effect” and the dynamic response of the exchange biasing can be explained by a thermal fluctuation model in which the antiferromagnet is assumed to be composed of grains which undergo thermal fluctuations.

DOI: 10.1103/PhysRevB.64.184416

PACS number(s): 75.70.Cn, 75.30.Gw, 75.60.Ej, 75.50.Ss

I. INTRODUCTION

The exchange bias effect, which arises from the interfacial exchange coupling between a ferromagnet (FM) and an antiferromagnet (AF), was discovered more than 40 years ago.¹ It is so named because the phenomenon manifests itself in a shifted hysteresis loop for the bilayer film. The exchange field H_e is defined by the loop displacement. The quantity $H_e M_s t_F$, where M_s and t_F are the saturation magnetization and the thickness of the FM layer, respectively, is defined as the unidirectional exchange anisotropy. This product is generally independent of the FM thickness. There have been many studies of the exchange bias effect since its first observation.² Many of the theoretical studies that focused on the origin and the magnitude of the exchange anisotropy have considered the role of uncompensated or compensated interfaces,^{3–7} as well as single-crystal versus polycrystalline bilayers.^{8,9} The exchange biasing of a FM coupled with an AF is always accompanied with a coercivity enhancement, which has been attributed to switching^{3,10,11} of AF domains or the existence of an interfacial random field.¹² The FM/AF exchange coupling is of particular interest because of its role in pinning one of the FM layers in a giant magnetoresistive spin-valve head for high-density recording systems.¹³

Exchange biasing is strongly dependent on temperature. In most cases, the exchange field decreases with increasing temperature. Since the ambient temperature of a spin-valve head is increased by the bias current during reading operations, the thermal stability of the exchange biasing is of concern for head design and the choice of the biasing materials. There are also several other effects related to the thermal stability of exchange biasing. One is the “training effect,” i.e., a decrease of the exchange field and coercivity with consecutive measurement cycles. This was first reported^{14,15} by Paccard and co-workers in Co/CoO bilayers, and was later attributed to thermal fluctuations. The time, frequency, and field sweep rate dependencies of the exchange coupling in FM/AF bilayers have also been investigated.^{16–20} Fulcomer and Charap¹⁷ observed an increase of the exchange

field and an accompanying decrease of the coercivity with increasing applied field frequency in oxidized Permalloy films. They developed a thermal fluctuation model to explain the observed temperature and frequency dependence of the exchange bias and coercivity. But they did not treat the training effect. More recent studies^{19,20} on Mn-based biasing materials showed that the sweep rate responses of the exchange field and coercivity were dependent on composition as well as temperature. Another experiment observed the recovery of the exchange bias after it is reversed by a large applied field.²¹

Stiles and McMichael²² and Stamps²³ extended the model of Fulcomer and Charap by considering planar domain wall formation and spin-flop coupling, respectively.^{22,23} McMichael *et al.* recognized that the difference in the time it takes to perform a hysteresis loop measurement compared with the thermal relaxation time of the AF grains can lead to time dependent exchange bias.²⁴ In this paper, we measure the dependence of the exchange bias and coercivity on many variables such as frequency, thickness of the AF, maximum field strength, and number of field cycles in the exchange coupled $\text{Ni}_{81}\text{Fe}_{19}/\text{Ir}_{22}\text{Mn}_{78}$ bilayer system. Studying all these dependencies in one system enables us to confirm the importance of the AF grains in the exchange bias phenomenon.

II. EXPERIMENT

$\text{Ni}_{81}\text{Fe}_{19}/\text{Ir}_{22}\text{Mn}_{78}$ bilayer samples were sequentially deposited by rf magnetron sputtering onto oxidized silicon substrates with a seedlayer in a SFI sputtering system. A 40-Å metallic cap layer was deposited on top of the $\text{Ir}_{22}\text{Mn}_{78}$ layer to protect the samples against oxidation in air. The base pressure of the sputtering system was typically 10^{-8} Torr. The $\text{Ni}_{81}\text{Fe}_{19}$ and $\text{Ir}_{22}\text{Mn}_{78}$ films were sputtered from a Permalloy and an IrMn alloy target, respectively. The deposition rates were about a fraction of 1 Å per second. The unidirectional exchange anisotropy and the uniaxial anisotropy of the exchange-coupled $\text{Ni}_{81}\text{Fe}_{19}$ layer were induced by a magnetic field in the sputtering chamber during deposition. One

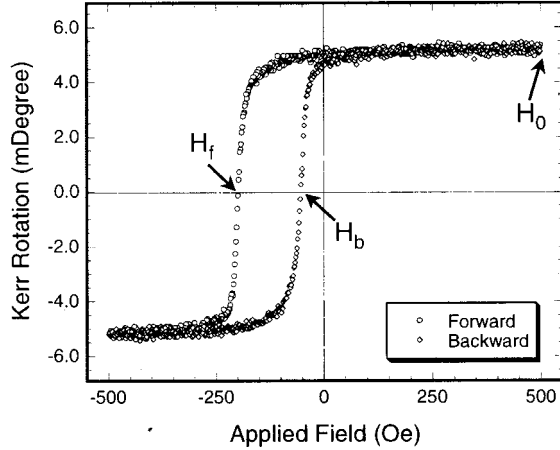


FIG. 1. Representative easy-axis hysteresis loop obtained from MOKE measurement on a $\text{Ni}_{81}\text{Fe}_{19}$ (60 Å)/ $\text{Ir}_{22}\text{Mn}_{78}$ (25 Å) bilayer with a field sweep rate of 1000 Oe/sec. The data were taken in the first cycle of measurements.

of the advantages of $\text{Ir}_{22}\text{Mn}_{78}$ in a device is that it does not have to be annealed to exhibit exchange bias.

The composition of the IrMn films was measured by energy dispersion x-ray fluorescence. The crystallographic structure of the polycrystalline samples was determined using x-ray diffraction. A face-centered-cubic (fcc) structure with (111) texture was found for $\text{Ni}_{81}\text{Fe}_{19}$ layer. The $\text{Ir}_{22}\text{Mn}_{78}$ films, deposited on the underlying $\text{Ni}_{81}\text{Fe}_{19}$ film, were found to have a γ phase of a disordered fcc structure, with a strong (111) texture. Although the composition ratio of Mn to Ir is very close to 3:1, there was little evidence or the existence of the ordered γ' phase with the Cu_3Au structure. Cross-section transmission electron microscopy measurements showed that the grain size of the $\text{Ir}_{22}\text{Mn}_{78}$ films was in the range of 300–500 Å.

Hysteresis loops were measured at room temperature using magneto-optic Kerr effect (MOKE) microscopy. Each full hysteresis loop with more than 5000 measurement points and a field sensitivity of 0.1 Oe was performed on a DMS wafer mapping system. The dimension of the laser beam spot was about 2 mm, which was smaller than the variations across the wafer.

III. RESULTS AND DISCUSSION

Figure 1 shows a representative hysteresis loop obtained by MOKE measurement. To obtain this loop took 1 sec for the applied field to sweep from H_0 , which we call the “field strength” down to $-H_0$. The field, H_f , where the observed magnetization decreases to zero is labeled as the “forward” coercivity. The applied field was maintained at $-H_0$ for 0.5 sec, which was half the field sweep time from H_0 to $-H_0$ before it was cycled through H_b , the “backward” coercivity, and increased back to H_0 . This reversal process took 1 sec and stayed at H_0 for another 0.5 sec before the full loop was repeated. In this experimental scheme the field sweep rate r_s

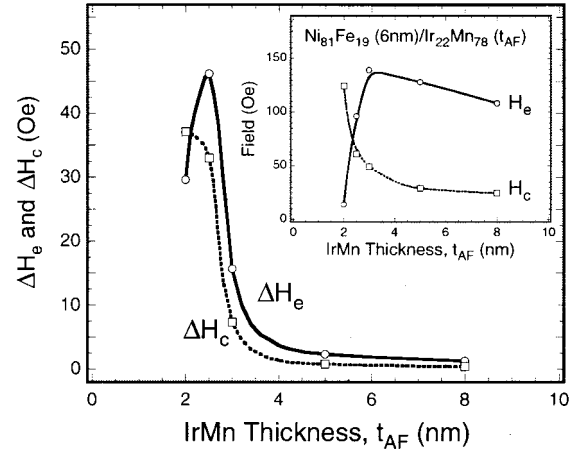


FIG. 2. Decreases of the exchange field and the coercivity, ΔH_e and ΔH_c , respectively, after 50 cycles of measurements under an applied field sweep rate of 1000 Oe/sec for samples with $\text{Ni}_{81}\text{Fe}_{19}$ layer thicknesses of 20, 25, 30, 50, and 80 Å. Inset is the $\text{Ir}_{22}\text{Mn}_{78}$ thickness dependence of the exchange field H_e and the coercivity H_c after 50 cycles of measurements.

is related to the loop measurement time τ_{hl} by $r_s = 6H_0/\tau_{hl}$.

Most studies of exchange bias focus on the exchange field H_e and the coercivity H_c . In this paper we shall study the effect of thermal fluctuations on the forward coercivity H_f and the backward coercivity H_b . The parameter set (H_e, H_c) is related to (H_f, H_b) by $H_f = H_e + H_c$ and $H_b = H_e - H_c$.

A. Training effect and thickness dependence

It is well known that the exchange field decreases very rapidly with AF thickness when the AF layer becomes thinner than a critical value. The coercivity also increases rapidly with decreasing thickness below this value. The inset of Fig. 2 shows a typical AF thickness dependence of the exchange field and coercivity. The gradual decrease of the exchange field with increasing $\text{Ir}_{22}\text{Mn}_{78}$ thickness when the $\text{Ir}_{22}\text{Mn}_{78}$ thickness is larger than 30 Å, shown in the inset, is also found in other biased systems.²⁵ This decrease is associated with the decrease of the AF domain size,²⁶ or the AF grain size, with thickness for a polycrystalline bilayer.

Several effects associated with the AF thickness (t_{AF}) have been found: the rotational hysteresis loss is found to have a peak as a function of t_{AF} ; (Ref. 27); the ferromagnetic resonance (FMR) field shows a negative shift with t_{AF} , the FMR linewidth broadens in the critical thickness region,^{28–30} and the angular dependence of the exchange field obtained from loop measurements shows asymmetry in the critical thickness region.³¹ All the phenomena above have been related to the AF domains or grains, in which thermal fluctuations plays a role.²²

Figure 2 shows the decrease of the exchange field and coercivity after 50 consecutive cycles of loop measurements. We see that the training effect is very large in the samples

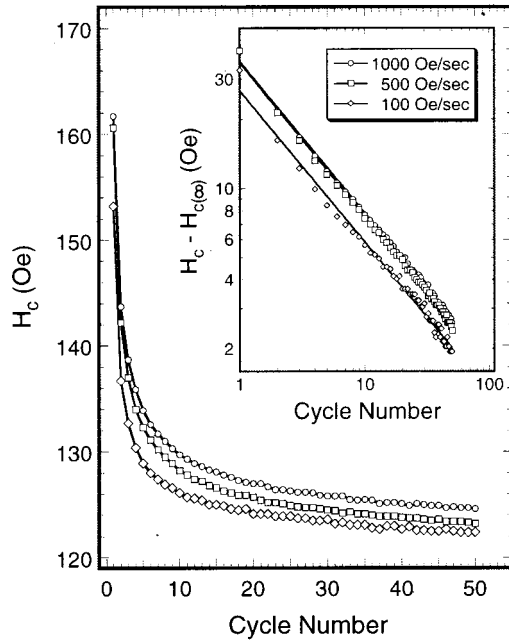


FIG. 3. Coercivity H_c vs cycle number n of measurements with field sweep rates of 100, 500, and 1000 Oe/sec for the $\text{Ni}_{81}\text{Fe}_{19}$ (60 Å)/ $\text{Ir}_{22}\text{Mn}_{78}$ (20 Å) bilayer. The inset shows a power-law relationship between the coercivity and the cycle number.

with an $\text{Ir}_{22}\text{Mn}_{78}$ thickness in the critical region. For the sample with an 80-Å-thick $\text{Ir}_{22}\text{Mn}_{78}$ layer, the changes of the exchange field and coercivity “after 50 cycles of training” are less than 3 Oe, which is much smaller than the values of the exchange field and coercivity. Our study will concentrate on the samples with $\text{Ir}_{22}\text{Mn}_{78}$ thicknesses of 20, 25, 30, and 50 Å.

The decrease of the exchange field and coercivity with the measurement cycles can be quantified. Paccard and co-workers^{14,15} were the first to analyze the training behavior in detail. For the system Co/CoO, they proposed power-law functions for the coercivities H_f and H_b on the cycle number n . Rewriting those for the coercivity H_c and the exchange field H_e ,

$$H_c(n) = H_{c(\infty)} + D_c n^{-\alpha}, \quad (1a)$$

$$H_e(n) = H_{e(\infty)} + D_e n^{-\beta}, \quad (1b)$$

where α and β are power indices which are always positive, and $H_{c(\infty)}$ and $H_{e(\infty)}$ are the limiting values referring to an infinite number of cycles for H_c and H_e , respectively. Recently Hung *et al.*³² described the cycle dependence of the exchange field by an expression analogous to that for the time dependence of the coercivity obtained by Sharrock.³³ However, the experimental data are not well described by this formula. Therefore, let us try fitting our data to Eq. (1). As shown in Figs. 3 and 4 for the sample with a 20-Å-thick

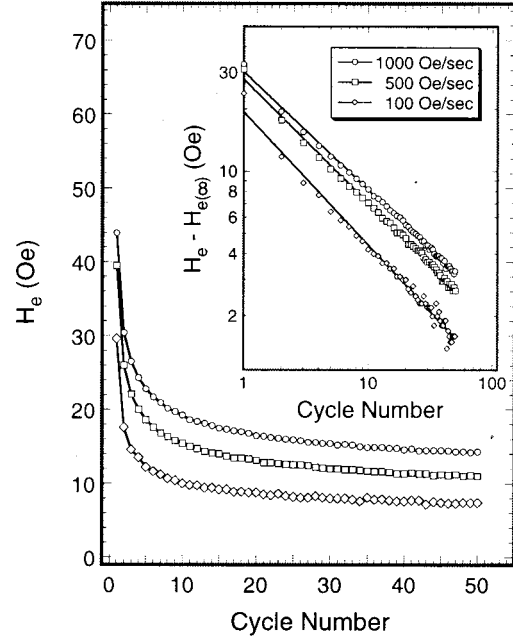


FIG. 4. Exchange field H_e vs cycle number n of measurements with field sweep rates of 100, 500, and 1000 Oe/sec for the $\text{Ni}_{81}\text{Fe}_{19}$ (60 Å)/ $\text{Ir}_{22}\text{Mn}_{78}$ (20 Å) bilayer. The inset shows a power-law relationship between the exchange field and the cycle number.

$\text{Ir}_{22}\text{Mn}_{78}$ layer, the coercivity and exchange field follow power-law relationships with the measurement cycle number very well.

All the power indices and limiting values can be obtained by fitting the formula to the experimental data. Consider the $\text{Ni}_{81}\text{Fe}_{19}$ (60 Å)/ $\text{Ir}_{22}\text{Mn}_{78}$ (20 Å) bilayer. α and β for the coercivity and exchange field at a field sweep rate of 100 Oe/sec are 0.667 and 0.683, respectively. Note that these values are defined differently from those of Paccard and co-workers in Co/CoO bilayers by a factor of 1/2.^{14,15} The value of α does not change much with the field sweep rate from 100 to 1000 Oe/sec, while β decreases from 0.683 to 0.571. The training curves of the coercivity and exchange field show that for a given cycle number n , $H_c(n)$ and $H_e(n)$ give larger values when the field sweep rate is higher. One might think that since the loop measurement takes a longer time for a lower sweep rate, it would be better to study the training of coercivity and exchange field with respect to the measurement time. However, the limiting values, $H_{c(\infty)}$ and $H_{e(\infty)}$, which are independent of the measurement time τ_{hl} show different values for different sweep rates, suggesting that the training behavior is field sweep rate dependent (recall that the sweep rate $r_s = 6H_0/\tau_{hl}$). We shall discuss this below.

The training results in a decrease of the exchange field and a “contraction” of the hysteresis loop. In reality, the forward coercivity H_f decreases with the number of measurement cycles while the backward coercivity H_b decreases in the first several cycles and then does not change much for the remaining cycles.³⁴ We also find that the coercivity and exchange field of the first loop do not fit the formula. The

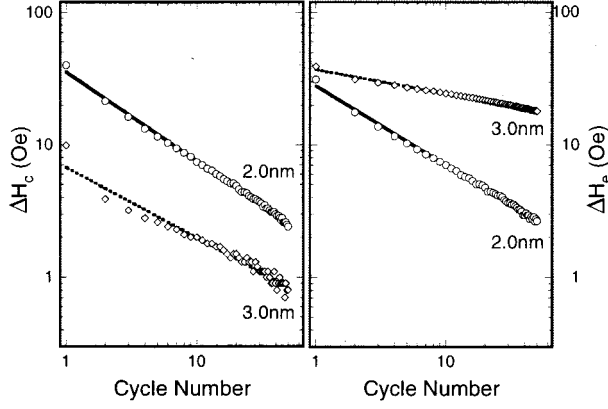


FIG. 5. Comparison of the dependencies of the exchange fields and the coercivities on the cycle number for the samples of 20- and 30-Å $\text{Ir}_{22}\text{Mn}_{78}$ layers. The numbers in the plot indicate the $\text{Ir}_{22}\text{Mn}_{78}$ thicknesses.

change in the first cycle was argued to be proportionally related to the rotational hysteresis loss of the bilayer.^{3,15} However, the reason to that the first cycle does not fit the power law relationship is still unknown.

In our $\text{Ni}_{81}\text{Fe}_{19}/\text{Ir}_{22}\text{Mn}_{78}$ bilayer system, the training behavior, as characterized by the power indices and the limiting values, are dependent not only on the field sweep rate but also on the $\text{Ir}_{22}\text{Mn}_{78}$ layer thickness. A comparison of the training of the coercivity and exchange field between the samples with 20-Å and 30-Å $\text{Ir}_{22}\text{Mn}_{78}$ layers is shown in Fig. 5. The 30-Å $\text{Ir}_{22}\text{Mn}_{78}$ sample shows slower training of H_c and H_e with the number of cycles than the 20-Å $\text{Ir}_{22}\text{Mn}_{78}$ sample does. In fact, the power-law indices become smaller with increasing $\text{Ir}_{22}\text{Mn}_{78}$ thickness.

B. Thermal fluctuation mechanism

To determine the effect of thermal fluctuations on exchange bias in a polycrystalline FM/AF bilayer, Fulcomer and Charap employed a “superparamagnetism” model,¹⁷ in which the AF layer is approximated by an assembly of grains without intergrain exchange coupling that extend through the thickness t_{AF} . This model is illustrated in Fig. 6. It is also assumed that the grains are all the same size and their easy axes are all in the same direction. Each grain is assumed to have a net moment \mathbf{m} at its interface with the FM. This may be the result of an uncompensated interface on the result of surface roughness. Suppose that the AF grains are ferromagnetically exchange coupled to the FM magnetization \mathbf{M}_{FM} at the interface by a strength J_0 . Let the number of grains whose surface moment is parallel (antiparallel) to the FM magnetization be n_+ (n_-). The effects we are describing are associated with fluctuation of these AF grains. The time τ_{\pm} for a grain to overcome an energy barrier $\Delta E_{\pm}S$ and switch to another energy state at a temperature T is given by

$$\frac{1}{\tau_{\pm}} = \nu_0 \exp\left(-\frac{\Delta E_{\pm}S}{k_B T}\right), \quad (2)$$

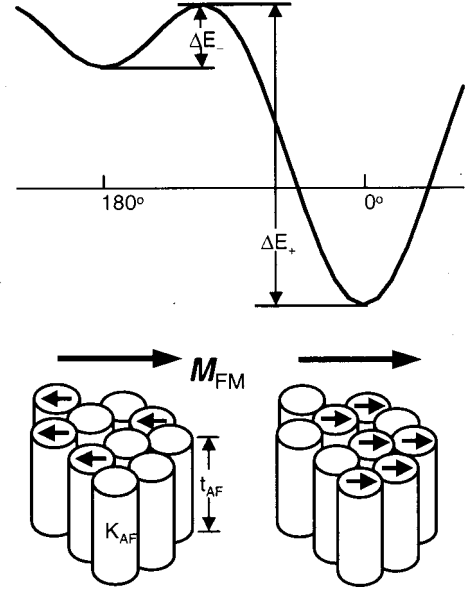


FIG. 6. Schematic representation of the energy states of the AF grains exchange coupled with the FM magnetization \mathbf{M}_{FM} at the interface. For convenience, the columnar AF grains are simply identical with a cross area of S , a length of t_{AF} , and a uniaxial anisotropy constant of K_{AF} . By considering the net moments point right or left at the interface, the AF grains are separated into two groups with a population fraction of n_+ and n_- , respectively. For the case that \mathbf{M}_{FM} points to right, i.e., with an angle of 0° , two stable states are shown and the barrier energies for the AF grains are ΔE_+ and ΔE_- , respectively. As \mathbf{M}_{FM} reverses, the energy states flip over correspondingly.

where ν_0 is the precession frequency of magnetic moments of the order of 10^9 sec^{-1} and k_B is the Boltzmann constant. A system composed of grains with just two energy states will take a time τ_0 ,

$$\frac{1}{\tau_0} = \frac{1}{\tau_+} + \frac{1}{\tau_-}, \quad (3)$$

to thermally relax from nonequilibrium to equilibrium. The barrier energies ΔE_+ and ΔE_- , normalized to the unit area, are related to the interfacial coupling J_0 and the internal energy of the AF grains. Stiles and McMichael²² considered the formation of a planar domain wall in the AF grains in their theoretical study, and Stamps²³ considered spin-flop coupling as well. However, since the $\text{Ir}_{22}\text{Mn}_{78}$ thicknesses of the samples in our study are very thin, we shall neglect these possibilities and assume a coherent rotation of the AF grains during switching and apply the formula of Fulcomer and Charap.¹⁷ For the barrier energies we take

$$\Delta E_{\pm} = K_{\text{AF}} t_{\text{AF}} \left[1 + \left(\frac{J_0}{2K_{\text{AB}} t_{\text{AB}}} \right)^2 \right] \pm J_0 \quad (4)$$

It is easy to demonstrate that for $J_0 < 2K_{\text{AF}} t_{\text{AF}}$ the barrier energies increase with increasing AF thickness t_{AF} , given

that K_{AF} is constant. For $J_0 > 2K_{AF}t_{AF}$, there is no energy barrier and the grains will relax to equilibrium rapidly.

Note that the grain relaxation is independent of the external field. This independence was confirmed in the experiments of the reversal of the exchange biasing by van der Heijden *et al.*²¹ However, the energy state of the grains depends on the interface net moment alignment with respect to the FM magnetization, which is driven by the external applied field. At a given time, the total energy of the bilayer is the sum of the exchange coupling energies of the grains. The total coupling energy per unit area of the bilayer is given by

$$J_E = J_0(n_+ - n_-). \quad (5)$$

Khapikov *et al.*³⁴ established complicated formulas for the coercivities in hysteresis loop measurements. We will simply use $H_{f(b)} = J_E / M_{FM}t_{FM}$, where J_E is given by Eq. (5) and t_{FM} is the FM thickness, to illustrate the training effect. Therefore, H_f and H_b are dependent on the population difference between the two groups of the AF grains whose interface uncompensated moments are parallel or antiparallel to the FM magnetization at the time when forward and backward reversals of the FM occur, respectively.

At the beginning of a loop measurement, the population of each grain group does not change until the FM magnetization reverses direction. When the magnetization is reversed by the applied field, the AF grains “see” a different energy barrier and then relaxation occurs. The bilayer will become biased in the opposite direction if the FM magnetization is kept in the reversed state ($-H_0$) for an infinite time. However, for consecutive loop measurements the applied field is driven back and forth. After a finite time at $-H_0$ the grain population will have changed, resulting in a different field H_b at which the magnetization reverses back to its original direction. To the extent that this relaxation is not completed, each subsequent measurement occurs with the grains out of thermodynamic equilibrium. Since the numbers of the grains in the two groups get close to each other in the presence of an oscillating applied field, the exchange field and the coercivity decrease with each cycle.

The changes in the coercivity and the exchange field during training are dependent on the grain relaxation rate with respect to the field sweep rate. The relaxation rate, in turn, decreases with the AF thickness. Figure 5 shows that the bilayer of 30-Å $\text{Ir}_{22}\text{Mn}_{78}$ gives a slower decay of the coercivity and the exchange field with the cycle number than the 20-Å $\text{Ir}_{22}\text{Mn}_{78}$ sample does. Due to a slow relaxation rate, there is a large separation between the limiting value and the value after 50 cycles of the exchange field for the sample of 30-Å $\text{Ir}_{22}\text{Mn}_{78}$. However, the coercivity, which changes little with training, is very close to its limiting value after 50 cycles.

In reality, polycrystalline bilayers are comprised of AF grains with different sizes and different anisotropy directions. In addition, the interfacial exchange coupling strength varies from grain to grain. Grains with $J_0 > 2K_{AF}t_{AF}$, i.e., small grains, exhibit a coercivity which is independent of the sweep rate. Grains with $J_0 < 2K_{AF}t_{AF}$ give both coercivity and exchange biasing with relative importance depending on

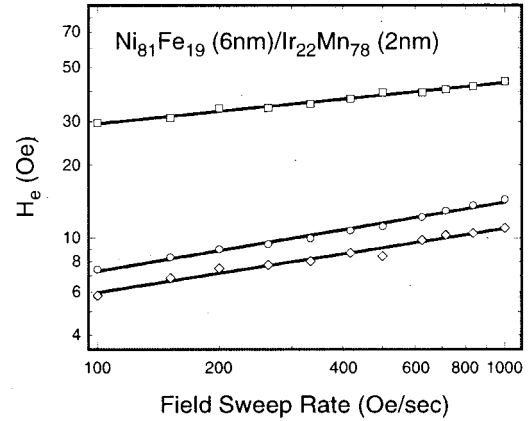


FIG. 7. Exchange fields vs applied field sweep rate of the $\text{Ni}_{81}\text{Fe}_{19}$ (60 Å)/ $\text{Ir}_{22}\text{Mn}_{78}$ (20 Å) bilayer. The data (□) show the exchange field obtained from the first loop. The data (○) are the averaging of the exchange field of the last ten loops. The points (◇) are the limiting value $H_{e(\infty)}$ obtained by fitting the measured data to the power-law relationship.

size of the relaxation time relative to the measurement time.^{17,34} The main contribution to the training effect and the field sweep rate dependence comes from grains with a relaxation rate comparable with the measurement rate.

C. Sweep rate dependence

Measurements of the sweep rate r_s , dependence of the coercivity and exchange biasing have been made previously in several exchange biased systems including $\text{Ni}_{81}\text{Fe}_{19}/\text{Ir}_{22}\text{Mn}_{78}$ bilayers.^{19,20} Since exchange-biased systems are subject to the training effect, it is important to study the systems during the first loop as well as after training. To accomplish this, we carried out 50 consecutive loop measurements on each sample at a given sweep rate. The samples were then placed in a zero-field environment for at least 22 h so that the samples would return to their initial states before the next set of measurements. The loop measurements were carried out with a fixed field strength H_0 of 500 Oe and a field sweep rate r_s in a range of 100–1000 Oe/sec.

Figure 7 shows the sweep rate dependence of various exchange fields H_e for the $\text{Ni}_{81}\text{Fe}_{19}$ (60 Å)/ $\text{Ir}_{22}\text{Mn}_{78}$ (20 Å) bilayer. The exchange field can be described by the following power law:

$$H_e = H_{e0} r_s^\gamma. \quad (6)$$

The exchange field obtained from the first loop has a power index of 0.1688. In fitting the experimental data to Eq. (6), we do not include a zero-sweep-rate value for the exchange field. The reason for this is that when the field sweep rate approaches zero, all the AF grains will have enough time to relax and then there will be no exchange bias in this limiting situation. The power indices for the exchange field averaged over the last 10 loops and the limiting value are 0.2835 and

0.2663, respectively. Since the values of these two parameters are rather close, we will use the averaged value for discussion.

Based on the discussion in Sec. III B, the forward coercivity H_f of the first loop measurement should be independent of the sweep rate. Stamps's Monte Carlo simulation on exchange biased systems gives such a result.²³ However, H_f was found to increase with increasing sweep rate in our $\text{Ni}_{81}\text{Fe}_{19}/\text{Ir}_{22}\text{Mn}_{78}$ bilayers.

Given the fact that magnetic films have complicated structures, various mechanisms contribute to the magnetization reversal and, hence, the coercivity. For a single polycrystalline FM film, the particlelike FM grains are under the influence of thermal fluctuations, and as a result the coercivity decays with time³³ and increases with the sweep rate.³⁵ A recent study of the magnetization reversal of polycrystalline $\text{Ni}_{80}\text{Fe}_{20}$ thin films in an oscillating external field with a frequency range of 1–800 Hz revealed a power-law dependence of the hysteresis loop area on the frequency and the field strength.³⁶ The dynamic magnetization reversals of the polycrystalline $\text{Ni}_{80}\text{Fe}_{20}$ films³⁶ and the epitaxial Fe films³⁷ were found to result from domain nucleation and domain-wall motion. A quasistatic study of the magnetization reversals in NiO/NiFe (Ref. 38), NiO/Co (Ref. 39), and MnF_2/Fe (Ref. 40) bilayers showed that the magnetization reversal and the FM domain nucleation of an exchange biased film could be asymmetric and more complicated than those of a nonbiased film. Furthermore, due to the interfacial random field, the FM domain size in an exchange-biased bilayer during magnetization reversals becomes small compared with a single FM layer and decreases with decreasing FM thickness.¹² The random field results in an enhanced coercivity H_c as well. All these effects should be taken into account in a study of the dynamic magnetization reversal in the exchange biased systems.

The forward coercivity H_f continues to increase with increasing sweep rate after repeated cycling. Separating H_f into a coercivity contribution and an exchange field H_e , we obtain the sweep rate dependence of H_c and H_e for the samples with various $\text{Ir}_{22}\text{Mn}_{78}$ thicknesses, as shown in Fig. 8. The power-law increase of the exchange field with the sweep rate holds well for all samples. The power index γ is 0.2663, 0.0761, 0.0307, and 0.0036 for samples with 20-, 25-, 30-, and 50-Å $\text{Ir}_{22}\text{Mn}_{78}$, respectively, suggesting a decrease with increasing $\text{Ir}_{22}\text{Mn}_{78}$ thickness. On the other hand, the coercivity shows little change with the sweep rate, in contrast to the experimental observations in the oxidized NiFe systems¹⁷ and to the Monte Carlo simulations.²³ Instead of decreasing with increasing sweep rate as argued in Refs. 17 and 23, the coercivity for 20-Å $\text{Ir}_{22}\text{Mn}_{78}$ increases slightly with the sweep rate.

When the $\text{Ir}_{22}\text{Mn}_{78}$ layer is thick, like 50 and 80 Å, and the training effect is small, the exchange field and coercivity are almost independent of the sweep rate in the range of measurements. This result is consistent with that of as-deposited NiFe/IrMn films reported previously.²⁰ As the AF thickness increases, the uniaxial energy of the AF grains also increases, which decreases the relaxation rate, according to Eqs. (2) and (4). The sweep rate is then orders of magnitude

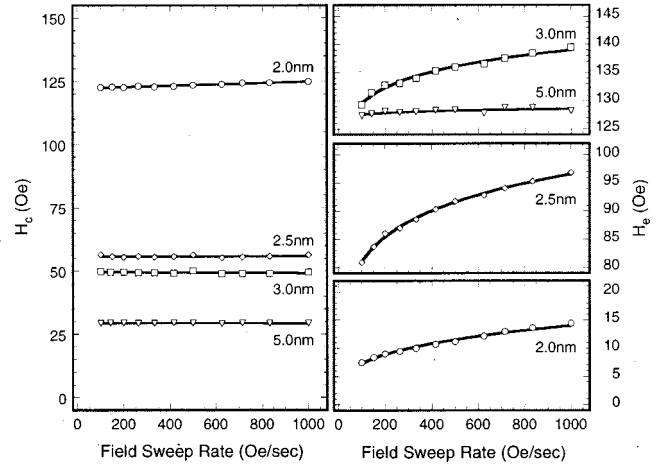


FIG. 8. Dependencies of the exchange field and the coercivity on the field sweep rate. The numbers close to the data in plot indicate the $\text{Ir}_{22}\text{Mn}_{78}$ thicknesses of the corresponding samples. The data are averaged over the last ten loops.

larger than the relaxation rate. The AF grains are virtually “frozen” during a loop measurement, resulting in an exchange field independent of the sweep rate.

It should be pointed out that the dynamic response of the exchange biasing and coercivity in thermally annealed samples is quite different from that of as-deposited films. Annealed IrMn/NiFe , $\text{PdPtMn}/\text{NiFe}$, and NiMn/NiFe samples were reported to exhibit a coercivity that increased noticeably with the sweep rate while the exchange field stayed almost constant.^{19,20} It is well known that the coercivity of an exchange biased FM increases with post-deposition annealing. A major effect of thermal annealing on bilayer and multilayer thin films is the interfacial diffusion, which leads to atomic mixing at the interface. The local exchange coupling at the FM/AF interface varies widely for a sample after annealing treatment. This can influence the FM domain structures during magnetization reversals. In addition, the “pinning” sites resulting from atomic mixing affect the domain wall motion of the FM layer.²⁰ These complications influence the dynamic magnetization reversals of the exchange-biased FM, giving a coercivity that is dependent on the FM layer, the AF layer, and the interface, and are beyond any simple theoretical analyses.

D. Field strength dependence

The effect of the field strength dependence on the training effect was studied by fixing the loop measurement time at 3 sec and changing the field strength H_0 within a range of 250–500 Oe.

The coercivity H_c of the $\text{Ni}_{81}\text{Fe}_{19}$ (60 Å)/ $\text{Ir}_{22}\text{Mn}_{78}$ (20 Å) bilayer decreases with a power-law behavior of the number of cycles. The power index was found to decrease from 0.851 to 0.663 with increasing field strength. Measurement results of the loop area, the coercivity, and the exchange field are shown in Fig. 9. The hysteresis loop area and the coercivity H_c show a linear increase with increasing field strength in the measurement range. Since the applied field is

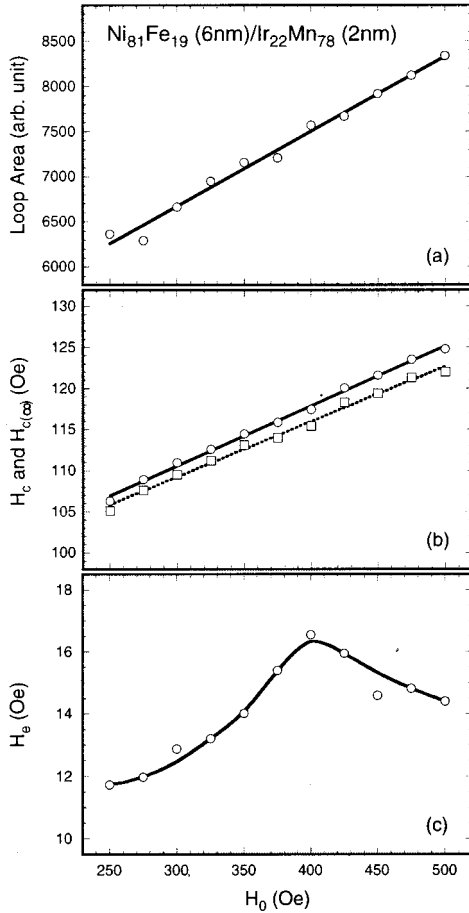


FIG. 9. Loop area A , coercivity H_c , and exchange field H_e vs the field strength H_0 of the $\text{Ni}_{81}\text{Fe}_{19}$ (60 Å)/ $\text{Ir}_{22}\text{Mn}_{78}$ (25 Å) bilayer. The data (○) are averaged over the last ten loops. The data (□) show the parameter $H_{c(\infty)}$ obtained from the power-law relationship.

less than five times as large as the coercivity, the magnetization is possibly not saturated in the loop measurements. The ratio of the loop area to the coercivity increases by about 13% for the field strength increasing from 250 to 500 Oe, supporting this speculation. For this sample the coercivity comes from the irreversible transition of the AF grains. A smaller coercivity at a lower field strength therefore means that fewer AF grains make irreversible transitions during the field sweep. The exchange field shows a peak as a function of field strength at 400 Oe. This is not understandable at present.

The loop measurement time is fixed, and, therefore, the time for grain relaxation is almost constant while the field strength is changed. This results in an almost constant exchange field. The samples other than the 20-Å $\text{Ir}_{22}\text{Mn}_{78}$ show a slight decrease, as shown in Fig. 10. The coercivity H_c increases slightly with the field strength. The increase of the coercivity as well as the decrease of the exchange field is dependent on the $\text{Ir}_{22}\text{Mn}_{78}$ thickness.

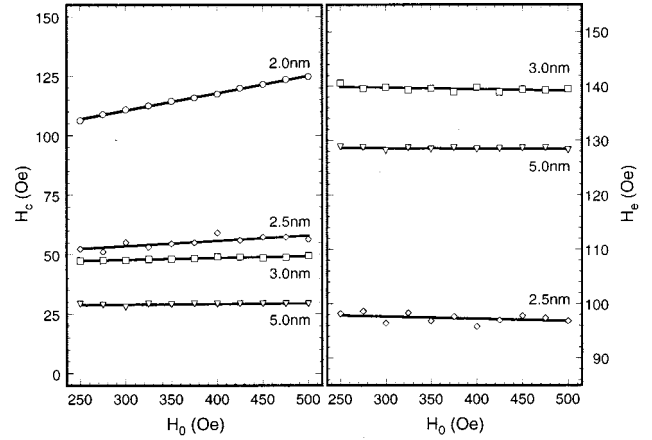


FIG. 10. Dependencies of the exchange field and the coercivity on the field strength H_0 . The numbers close to the data in plot indicate the $\text{Ir}_{22}\text{Mn}_{78}$ thicknesses of the corresponding samples. The data are averaged over the last ten loops.

E. Coercivity along the hard axis

The $\text{Ni}_{81}\text{Fe}_{19}$ (60 Å)/ $\text{Ir}_{22}\text{Mn}_{78}$ (20 Å) bilayer gives not only a large coercivity along the easy axis but also a large coercivity along the hard axis. The dispersion of the AF grain anisotropy orientations plays a role in the magnetization reversal along the easy axis. Since the $\text{Ir}_{22}\text{Mn}_{78}$ layer is very thin, most of the AF grains rotate irreversibly with the magnetization. Therefore, the observed coercivity along the hard axis is a reflection of the uniaxial anisotropy of the AF grains. The magnetization reversal behavior of the exchange-

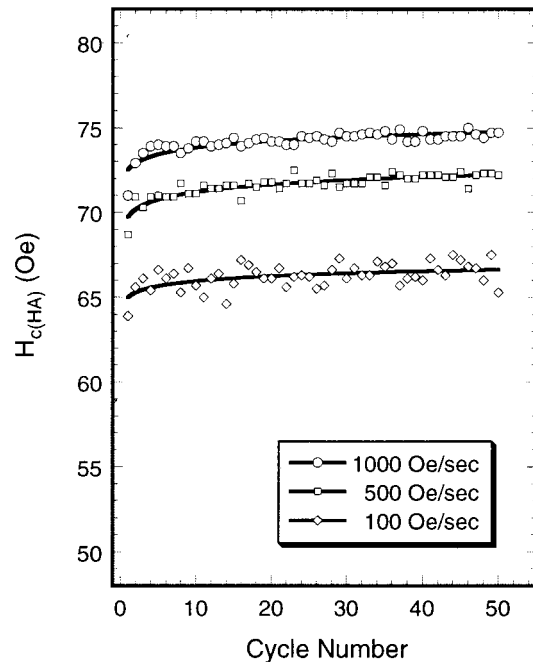


FIG. 11. Hard-axis coercivity $H_{c(\text{HA})}$ vs cycle number n of measurements with field sweep rates of 100, 500, and 1000 Oe/sec for the $\text{Ni}_{81}\text{Fe}_{19}$ (60 Å)/ $\text{Ir}_{22}\text{Mn}_{78}$ (20 Å) bilayer.

coupled FM layer to some degree resembles that of a system of Stoner-Wohlfarth particles, which are free of interparticle coupling and have randomly oriented anisotropies.

Figure 11 shows that the training of the sample with an oscillating field applied along the hard axis results in a slight increase in the coercivity $H_{c(\text{HA})}$ with the cycle number. We know that the training produces an out-of-equilibrium state in the bilayer in which the population difference of AF grains with uncompensated moments pointing in opposite directions decreases. This leads to a decrease in the exchange field. The increase of $H_{c(\text{HA})}$ after cycling measurements would then be associated with the decrease of the exchange biasing H_e along the easy axis. Again, this is analogous to a Stoner-Wohlfarth particle system with an external field applied perpendicular to the measurement direction; the measured coercivity increases with decreasing transverse bias field.

In addition, Fig. 11 shows that the hard-axis coercivity $H_{c(\text{HA})}$ increases with the sweep rate. In this case, the increase of $H_{c(\text{HA})}$ implies the involvements of the domain nucleation and the domain-wall motion during the magnetization reversal in the presence of a spatially varied coupling at the interface.

IV. SUMMARY

In this work, we have experimentally studied the hysteresis dynamics in exchange-coupled $\text{Ni}_{81}\text{Fe}_{19}/\text{Ir}_{22}\text{Mn}_{78}$ bilayers

at room temperature. Starting from the investigation of training effect in these bilayers, a thermal fluctuation model that was first proposed by Fulcomer and Charap,¹⁷ and recently updated and developed,^{22,23,34} is introduced. Qualitatively the field sweep rate dependence and the field strength dependence of the exchange biasing can be described within this model. We have also found that the exchange field increases with the sweep rate according to a power law in which the power index depends on the $\text{Ir}_{22}\text{Mn}_{78}$ thickness.

However, the increase of coercivity with the sweep rate cannot be explained by the thermal fluctuation model, which implies that the decrease of coercivity with the sweep rate matches the increase of exchange field. The observed dynamic behavior of coercivity suggests the involvement of domain nucleation and domain wall motion during the reversal of the FM magnetization, which is under the influence of interface random field.

ACKNOWLEDGMENTS

This work was supported in part by Seagate Technology, Inc. and by the National Science Foundation under Grant No. ECD-8907068. One of the authors (H.X.) thanks Dr. Jeffrey P. Treptau, Dr. Sheryl Foss-Schroeder, and John Hawkins for technical help, and Dr. Chouhong Hou, Dr. Jian Chen, and Dr. Eric Linville for helpful suggestions and discussion.

*Email address: hxi@andrew.cmu.edu

¹W. H. Meiklejohn and C. P. Bean, Phys. Rev. **102**, 1413 (1956); **105**, 904 (1957); W. H. Meiklejohn, J. Appl. Phys. **33**, 1328 (1962).

²For recent review articles, see J. Nogues and I. K. Schuller, J. Magn. Magn. Mater. **192**, 203 (1999); A. E. Berkowitz and K. Takano, *ibid.* **200**, 552 (1999).

³L. Néel, in *Selected Works of Louis Néel*, edited by N. Kurti (Gordon and Breach, New York, 1988), p. 469.

⁴D. Mauri, H. C. Siegmann, P. S. Bagus, and E. Kay, J. Appl. Phys. **62**, 3047 (1987).

⁵A. P. Malozemoff, Phys. Rev. B **35**, 3679 (1987); J. Appl. Phys. **63**, 3874 (1988).

⁶N. Koon, Phys. Rev. Lett. **78**, 4865 (1997).

⁷T. C. Schulthess and W. H. Butler, Phys. Rev. Lett. **81**, 4516 (1998); J. Appl. Phys. **85**, 5510 (1999).

⁸K. Takano, R. H. Kodama, A. E. Berkowitz, W. Cao, and G. Thomas, Phys. Rev. Lett. **79**, 1130 (1997); J. Appl. Phys. **83**, 6888 (1998).

⁹M. D. Stiles and R. D. McMichael, Phys. Rev. B **59**, 3722 (1999).

¹⁰I. S. Jacobs and C. P. Bean, in *Magnetism-III*, edited by G. T. Rado and H. Suhl (Academic, New York, 1963), p. 323.

¹¹H. Xi and R. M. White, Phys. Rev. B **61**, 80 (2000).

¹²S. Zhang, D. V. Dimitrov, G. C. Hadjipanayis, J. W. Cai, and C. L. Chien, J. Magn. Magn. Mater. **198–199**, 468 (1999); Z. Li and S. Zhang, Phys. Rev. B **61**, R14 897 (2000).

¹³D. Heim, R. Fontana, C. Tsang, V. Speriosu, B. Gurney, and M. Williams, IEEE Trans. Magn. **30**, 316 (1994); C. Tsang, R. E. Fontana, Jr., T. Lin, D. E. Heim, V. S. Speriosu, B. A. Gurney,

and M. L. Williams, **30**, 3801 (1994).

¹⁴D. Paccard, C. Schlenker, O. Massenet, R. Montmory, and A. Yelon, Phys. Rev. **16**, 301 (1966).

¹⁵C. Schlenker and D. Paccard, J. Phys. (Paris) **28**, 611 (1967).

¹⁶A. A. Glazer, A. P. Potapov, R. I. Tagirov, and Ya. S. Shur, Phys. Status Solidi **16**, 745 (1966).

¹⁷E. Fulcomer and S. H. Charap, J. Appl. Phys. **43**, 4184 (1972); **43**, 4190 (1972).

¹⁸A. M. Goodman, K. O. O'Grady, M. R. Parker, and S. Burkett, J. Magn. Magn. Mater. **193**, 504 (1999); A. M. Goodman, H. Laidler, K. O. O'Grady, N. W. Owen, and A. K. Petford-Long, J. Appl. Phys. **87**, 6409 (2000).

¹⁹Z. Yang, D. Hua, S. Mao, H. Wang, G. Al-Jumaily, P. J. Ryan, P. A. Crozier, S. Y. Tsen, M. McCartney, and M. Scheinfein, J. Appl. Phys. **87**, 5729 (2000).

²⁰S. Mao, Z. Yang, Z. Gao, D. Han, and T. Pokhil, IEEE Trans. Magn. **36**, 3056 (2000).

²¹P. A. A. van der Heijden, T. F. M. Maas, W. J. M. de Jonge, J. C. S. Kools, F. Roozeboom, and P. J. van der Zaag, Appl. Phys. Lett. **72**, 492 (1998); P. A. A. van der Heijden, T. F. M. Maas, J. C. S. Kools, F. Roozeboom, P. J. van der Zaag, and W. J. M. de Jonge, J. Appl. Phys. **83**, 7207 (1998).

²²M. D. Stiles and R. D. McMichael, Phys. Rev. B **60**, 12 950 (1999).

²³R. L. Stamps, Phys. Rev. B **61**, 12 174 (2000).

²⁴R. D. McMichael, C. G. Lee, M. D. Stiles, F. G. Serpa, P. J. Chen, and W. F. Egelhoff, Jr., J. Appl. Phys. **87**, 6406 (2000).

²⁵T. Ambrose and C. L. Chien, J. Appl. Phys. **83**, 6822 (1998); H. Sang, Y. W. Du, and C. L. Chien, *ibid.* **85**, 4931 (1999).

- ²⁶A. P. Malozemoff, Phys. Rev. B **37**, 7673 (1988).
- ²⁷S. Soeya, S. Nakamura, T. Imagawa, and S. Narishige, J. Appl. Phys. **77**, 5838 (1995).
- ²⁸W. Stocklein, S. S. P. Parkin, and J. C. Scott, Phys. Rev. B **38**, 6847 (1988).
- ²⁹R. D. McMichael, M. D. Stiles, P. J. Chen, and W. F. Egelhoff, Jr., Phys. Rev. B **58**, 8605 (1998).
- ³⁰H. Xi, K. R. Mountfield, and R. M. White, J. Appl. Phys. **87**, 4367 (2000).
- ³¹H. Xi and R. M. White, Phys. Rev. B **61**, 1318 (2000).
- ³²C.-Y. Hung, M. Mao, S. Funada, T. Schneider, L. Miloslavsky, M. Miller, C. Qian, and H.-C. Tong, J. Appl. Phys. **87**, 4915 (2000).
- ³³M. P. Sharrock, IEEE Trans. Magn. **26**, 193 (1990).
- ³⁴A. F. Khapikov, J. W. Harrell, H. Fujiwara, and C. Hou, J. Appl. Phys. **87**, 4954 (2000).
- ³⁵M. El-Hilo, A. M. deWitte, K. O'Grady, and R. W. Chantrell, J. Magn. Magn. Mater. **117**, 307 (1992).
- ³⁶B. C. Choi, W. Y. Lee, A. Samad, and J. A. C. Bland, Phys. Rev. B **60**, 11 906 (1999).
- ³⁷W. Y. Lee, Y. B. Xu, S. M. Gardiner, J. A. C. Bland, and B. C. Choi, J. Appl. Phys. **87**, 5926 (2000).
- ³⁸V. I. Nikitenko, V. S. Gornakov, L. M. Dedukh, Yu. P. Kabanov, A. F. Khapikov, A. J. Shapiro, R. D. Shull, A. Chaiken, and R. P. Michel, Phys. Rev. B **57**, R8111 (1998).
- ³⁹H. D. Chopra, D. X. Yang, P. J. Chen, H. J. Brown, L. J. Swartzendruber, and W. F. Egelhoff, Jr., Phys. Rev. B **61**, 15 312 (2000).
- ⁴⁰M. R. Fitzsimmons, P. Yashar, C. Leighton, I. V. Schuller, J. Nogués, C. F. Majkrzak, and J. A. Dura, Phys. Rev. Lett. **84**, 3986 (2000); C. Leighton, M. R. Fitzsimmons, P. Yashar, A. Hoffmann, J. Nogués, J. Dura, C. F. Majkrzak, and I. K. Schuller, *ibid.* **86**, 4394 (2001). C. Leighton and I. V. Schuller, Phys. Rev. B **63**, 174419 (2001).